Real-time Simulation of Underwater Acoustic Channels

Anton Namenas[1], Thorben Kaak[1], Gerhard Schmidt[1]

[1] *Digital Signal Processing and System Theory, Christian-Albrechts-Universität zu Kiel, Email: {ann, thka, gus}@tf.uni-kiel.de*

Abstract

Todays research interests in underwater communication and navigation are continuously growing. However, testing of new systems involves a lot of effort and costs. Due to this fact it is often useful to develop a complex simulation environment (SE).

The first aspect of the underwater channel simulation is closely related to the questions: What happens with an acoustic signal if it propagates through the water? And what kind of transformations are resulting from this?

Under water, there are a variety of effects which are influencing the propagation of the sound waves. This work deals with the real-time simulation of underwater signals for SONAR signal processing. The main focus lies in the implementation of an adaptive ray tracing method, which allows the simulation of time-varying multi-path propagation under the influence of a given sound velocity profile and other environmental properties such as the structure of the sea bottom or the sea surface.

Another feature of the simulation is the generation of spatially coherent noise signals with application to ambient sea noise in case of a multiple receiver system. Two special features of the simulation are the calculation of a time- and wind-dependent sea surface, as well as a possibility of using different sediment types and user-defined bottom surfaces. Another special feature of the SE is the hardware simulation, which allows the use of hardware-specific transmission functions like sensitivity curves of projectors and hydrophones.

Introduction

The sound propagation in an elastic medium such as water can be described mathematically by the wave equation. This type of description of a wave field is, however, very complex and can not be considered in real-time. A simplified solution of the wave equation, so-called ray tracing schemes can be used to describe the sound propagation in the sea with comparatively low computational effort. From a mathematical point of view, ray tracing is an initial value problem that can be solved with the explicit Euler method. Many published acoustic ray tracing methods are limited to two-dimensional environments [1, 2, 3], which reduces the computational effort but also limits the possibilities of the simulation. However, in order to use the advantages of a two-dimensional ray tracing, such as the relatively simple determination of the eigenrays, and at the same time to have diverse possibilities of the three-dimensional environment a two-plane solution was developed and implemented in this work. The two-plane solution is nothing else than separate viewing of the rays in the horizontal and vertical planes.

Underwater Simulation Environment

The main task of the underwater simulation environment (USE) is to determine the channels between the projectors and targets and between the targets and hydrophones, which are located in a defined underwater environment. The channels and projector signals are then used to generate hydrophone signals. The USE is divided into six modules which are connected to each other. The arrows represent the signal and parameter flow. Fig. 1 gives an overview of the system.
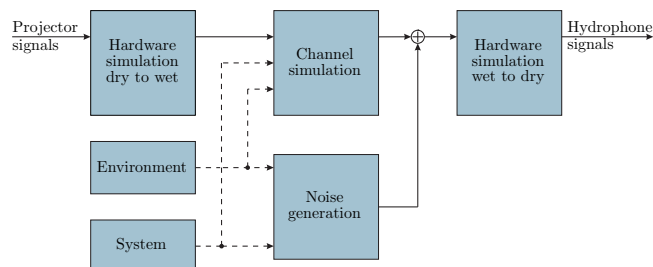

Figure 1: Block diagram of the USE.

Hardware Simulation

The first Hardware simulation (HS) module generates a sound pressure signal from a normalized projector signal. In the first step, the signal is converted into a voltage signal and then to a sound pressure signal by using the sensitivity curve of a projector, this is the so-called "dry to wet" path. Analogously to the first HS, there exists another HS module which describes the path of a sound signal to a normalized signal, this is the so-called "wet to dry" path.

Channel Simulation

The most important module of the USE is the channel simulation module, which consists of three ray tracing modules and two correlation modules, see Fig. 1 and 2.
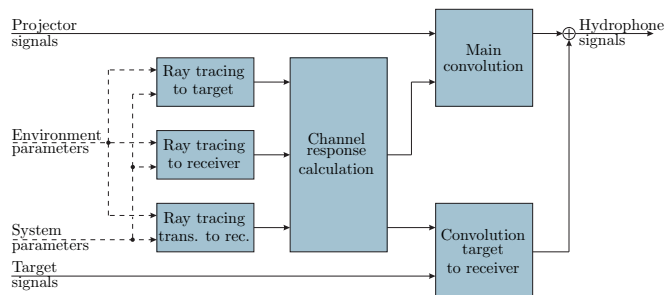

Figure 2: Block diagram of the channel simulation module.

The ray tracing modules calculate the paths which con-

nect the positions of the projectors, the targets, and the hydrophones with each other. The following parameters are also calculated for each of the paths:

- amplitude factor,
- traveling time,
- arc length,
- number of reflections,
- reflection angle, and
- number of caustics.

Ray tracing

Ray tracing is a purely geometric approach and can be described by the following differential equations [1, 2]:

$$\frac{dx}{ds} = \cos\beta\cos\alpha, \quad \frac{dy}{ds} = \cos\beta\sin\alpha, \quad \frac{dz}{ds} = -\sin\beta,$$

$$\frac{dr}{ds} = \cos\beta, \quad \frac{d\beta}{ds} = \frac{\cos\beta}{c}c', \quad \frac{dt}{ds} = \frac{1}{c}. \tag{1}$$

Where x, y, and z are the cartesian coordinates, s is the arc length, β the polar angle, α the azimuthal angle, c the sound velocity, t the traveling time and r the coordinate in the vertical plane, see Fig. 3.

As already mentioned, the ray tracing is first carried out in the horizontal plane and then in the vertical plane along the eigenrays of the horizontal plane, see Fig. 3. However, two assumptions have to be fulfilled for reliable operation. The first assumption is that the sound velocity is only dependent on the depth $c(z)$. This ensures that the rays remain in the considered plane. It is also assumed that the rays remain in the plane after reflection.
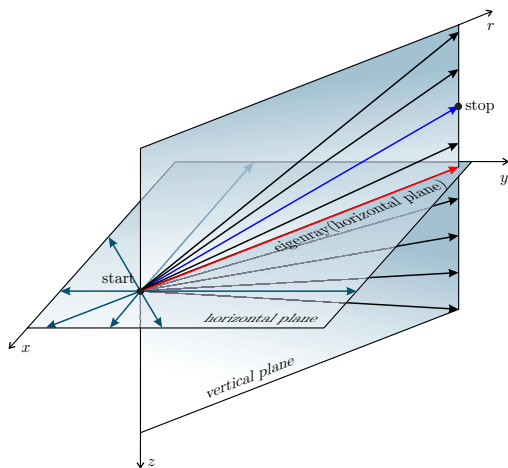
Figure 3: Two-dimensional ray tracing in three-dimensional space.

Eigenray Determination

An eigenray is defined as a ray that connects a source position with a receiver position. The determination of the eigenrays is the most difficult task in a ray tracing method. Nevertheless, due to the assumption that the sound velocity is only dependent on the depth and the

rays are moving either in the horizontal or vertical plane (see Fig. 3), the eigenrays or the eigenray initial angles can be determined relatively simple in a few steps. In the first step, a quantity of rays with different initial angles is defined in the horizontal plane. In the next step, the rays are tracked either up to the x-position or the y-position of the receiver to determine their y- and x-values at this point, respectively, see Fig. 4.
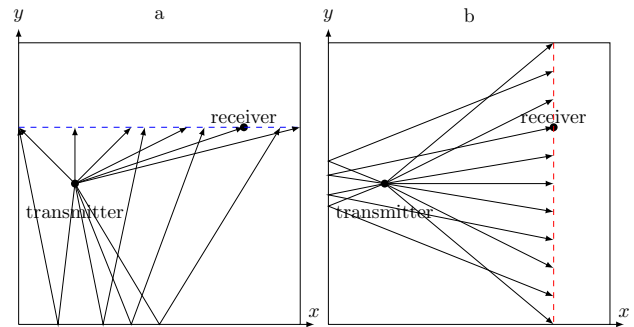
Figure 4: Determination of the *a:* x- and *b:* y-values for the detection of the eigenrays in the horizontal plane.

Fig. 5 shows an example of y- and x-values of the rays at the x- or y-position of a receiver in a (500 m × 500 m) xy-plane with reflective borders. It can be seen that the course of the values over the initial angle is relatively continuous and therefore amenable to interpolation. As expected, problem areas arise which are unsuitable for interpolation. This problem is due to the nearly parallel course of the rays to the y- or x-axis, see Fig. 5 gray marked areas. To overcome this problem, both variants are used to determine the eigenrays, however, not the entire area from 0° to 360°, but only the appropriate parts from this area.
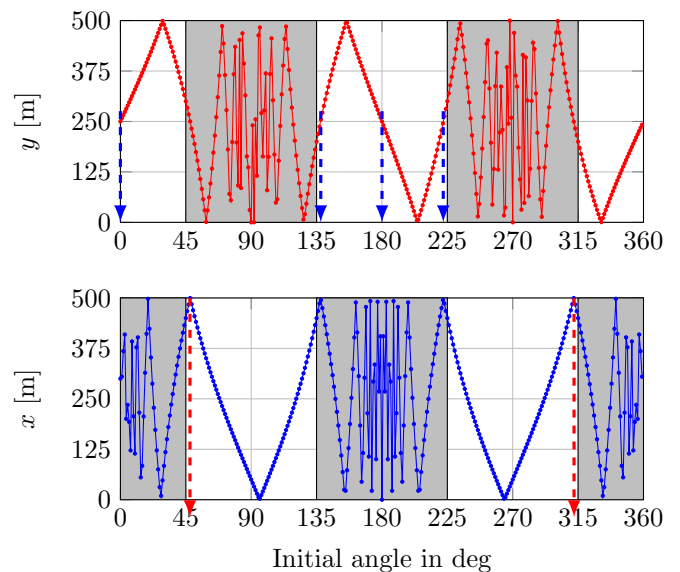
Figure 5: *Upper:* y- and *lower:* x-values of 361 rays at the x- and y-position of the receiver, respectively, as a function of the initial angle. The transmitter is located at the position (50 m, 250 m) and receiver at the position (500 m, 250 m).

Transmission Loss

The main contributions to the attenuation of an underwater acoustic wave are geometrical spreading, absorption, and reflections of the signals at the sea surface and bottom. Geometrical spreading TL_{geo} is due to the divergent behavior of the sound. The geometric spreading can be determined along a ray by equation (2) [4]:

$$TL_{\text{geo}} = 10 \log \left(\frac{c_n \cdot \cos(\beta_0) \cdot \Delta\beta_0 \cdot s_0^2}{c_0 \cdot r_n \cdot \Delta z \cdot \cos(\beta_n)} \right) \qquad \text{[dB]}. \tag{2}$$

Where c_n is the sound speed at the receiver, β_0 is the polar initial angle at the transmitter, $\Delta\beta_0$ is the polar opening angle at the transmitter, s_0 is the distance from the transmitter where the amplitude value is equal to one, c_0 is the sound speed at the transmitter, r_n is the distance to the receiver in the vertical plane, Δz is the height difference of neighboring rays, and β_n is the polar angle of the ray at the receiver, see Fig. 6
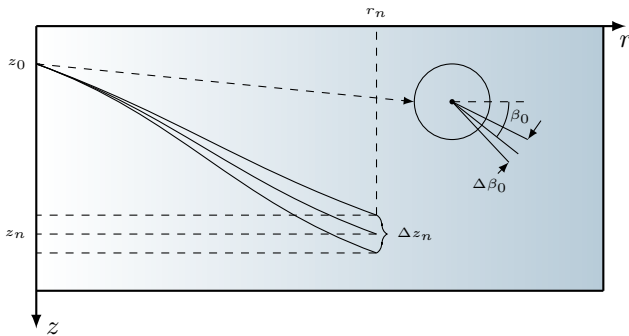
Figure 6: Geometry of three rays in the vertical plane.

In addition to the classical attenuation due to viscosity, liquids also have molecular absorption. The excitation of rotational and vibrational degrees of freedom of different molecules with a sound field leads to the loss of the translational energy and thus to an attenuation of the sound wave. The absorption loss TL_{abs} is given by equation (3), where a is the absorption coefficient, and s the distance traveled by the ray in meters:

$$TL_{\text{abs}} = a \cdot s \cdot 10^{-3} \qquad \text{[dB]}. \tag{3}$$

The model mainly used today to calculate the absorption coefficient a was proposed by Francois and Garrison [5]:

$$a = A_1 P_1 \frac{f_1 f^2}{f_1^2 + f^2} + A_2 P_2 \frac{f_2 f^2}{f_2^2 + f^2}$$
$$+ A_3 P_3 f^2 \quad \left[\text{dB} \cdot \text{km}^{-1} \right]. \tag{4}$$

A_i and P_i are coefficients that can depend on the salinity, pH, depth, temperature, and sound speed. f_1 and f_2 are the relaxation frequencies of boric acid and magnesium sulfate, respectively. f is the wave frequency. Another cause for attenuation are reflections at the borders in the water. The reflections at the sea surface or the sea bottom are usually dependent on the frequency of the sound

wave, the grazing angle γ_g, as well as the composition (density $\rho_{1,2}$ and sound speed $c_{1,2}$) and the texture of the surface . One of the simplest models for computing the bottom loss TL_{bott}, is the so-called Rayleigh model [6]. This model describes the sound reflection on the flat boundary layer of two media, in this case water and sea bottom:

$$TL_{\text{bott}} = 10 \log \left[\frac{q \sin(\gamma_g) - \sqrt{n^2 - \cos^2(\gamma_g)}}{q \sin(\gamma_g) - \sqrt{n^2 + \cos^2(\gamma_g)}} \right] \quad \text{[dB]}. \tag{5}$$

Where $q = \frac{\rho_2}{\rho_1}$ and $n = \frac{c_1}{c_2}$.

To determine the reflexion loss on the surface four empirical models are used:

- Rayleigh surface loss model [7],

- Modified Eckhart surface loss model [7],

- Schulkin-Marsh surface loss model [7],

- Beckmann-Spizzichino surface loss model [7].

Environment

The environment module contains of the common parameters of the simulated environment. These are e.g. physical dimensions of the surrounding environment, sound velocity profiles and much more. In addition to the common parameters, this module calculates the position of the targets depending on the speed and intermediate positions. Another important task of the module is the calculation of a discrete sea surface generated by the wind. The determination of the sea surface is realized with the inverse fast fourier transformation of the Phillips spectrum. For a more detailed description see [8].

Noise

Another important component of the USE is noise generation. The noise generation modul is depicted in Fig. 7. Four different empirical models are used to simulate ambient noise in the underwater environment [5, 9]: turbulence N_t, shipping N_s, wind N_w, and thermal noise N_{th}.
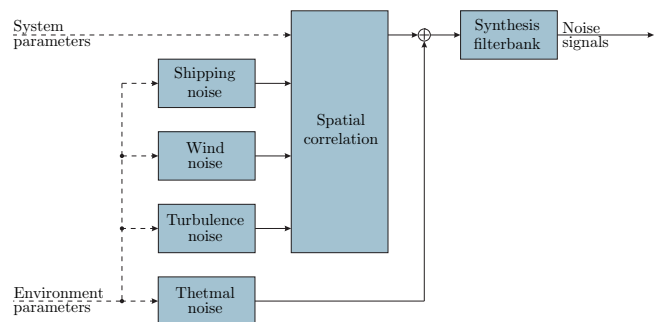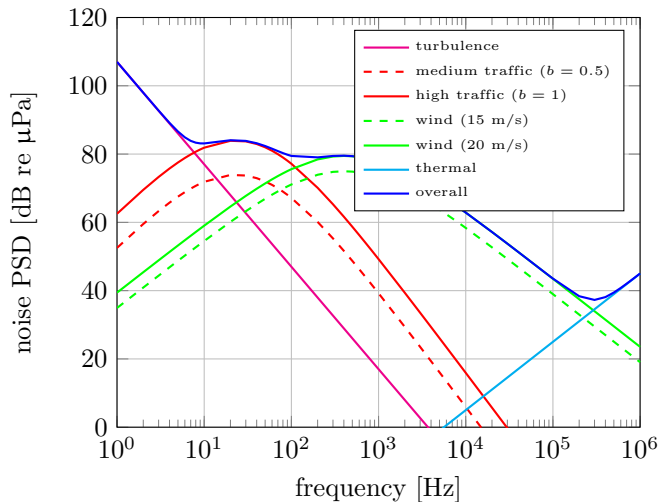

Figure 7: Block diagram of the Noise generation module.

The empirical models of the noise power spectral densitis are given by:

$$10 \log_{10} N_t(f) = 17 - 30 \log_{10}(f),$$
$$10 \log_{10} N_s(f) = 40 + 20(b - 0.5) + 26 \log_{10}(f)$$
$$- 60 \log_{10}(f + 0.03),$$
$$10 \log_{10} N_w(f) = 50 + 7.5\sqrt{v_w} + 20 \log_{10}(f)$$
$$- 40 \log_{10}(f + 0.4),$$
$$10 \log_{10} N_{th}(f) = -15 + 20 \log_{10}(f). \tag{6}$$

with frequency f in kHz, shipping activity $b \in [0, 1]$, and the wind speed v_w in m/s.

Figure 8: Power spectral density of various empirical noise models.

In addition to the different noise sources, the coherence between the noise signals of the hydrophones plays an important role [10, 11, 12]. The performance of a hydrophone array in a noise field depends on the cross-correlation function which describes the statistical relationships between all pairs of hydrophones in the array. This function depends on the geometry of the array and the directional properties of the noise field. To describe the coherence $\gamma_{pq}(f)$, the spherical isotropic noise fields and the anisotropic noise fields are considered in this work. Equation (7) describes the coherence between two hydrophones p and q in a spherical isotropic noise field with distance d_{pq}:

$$\gamma_{pq_{iso}}(f) = \frac{\sin(2\pi f d_{pq}/c)}{2\pi f d_{pq}/c}. \tag{7}$$

Equation (8) is used to describe the coherence in an anisotropic noise field caused by noise sources at the water surface. The array is parallel to the water surface. J_1 is a first-order Bessel function of the first kind.

$$\gamma_{pq_{aniso}}(f) = \frac{2 J_1(2\pi f d_{pq}/c)}{2\pi f d_{pq}/c}. \tag{8}$$

Conclusion and Outlook

This paper shows a complex USE for the simulation of sound propagation underwater with various environmental influences. The USE is specially adapted to the sonar signal processing and is able to describe the entire path of a sound wave from a projector to a hydrophone.

With regard to the completeness of the USE, it is also useful to create temperature and salinity profiles in addition to the sound velocity profiles. Furthermore, the use of target-specific backscatter coefficients should be considered. These are different in the case of different target bodies with respect to the angle of incidence and the frequency.

References

[1] A. Zielinski and X. Geng, *A new method for acoustic ray tracing*, Department of Electrical and Computer Engineering - University of Victoria, IEEE 1994.

[2] E. Svensson, *Physical modeling of acoustic shallow-water communication channels*, Doctoral Thesis, Stockholm, Sweden 2007

[3] J. M. Hovem, *Ray Trace Modeling of Underwater Sound Propagation*, Norwegian University of Science and Technology, 2008.

[4] H. Medwin, C.S. Clay, *Fundamentals of acoustical oceanography*, Academic Press, 1998.

[5] X. Lurton, *An Introduction to Underwater Acoustics - Principles and Applications*, Springer, 2002.

[6] NURC, *Sonar Acoustics Handbook*, La Spezia, Italy, 2009.

[7] R. P. Hodges, *Underwater Acoustics: Analysis, Design and Performance of Sonar*, Wiley, 2010.

[8] T. Liebmann, *Simulation von Wasser*, Universität Leipzig, Seminar Bild- und Signalverarbeitung, Wissenschaftliche Visualisierung, 2013.

[9] M. Stojanovic, *On the Relationship Between Capacity and Distance in an Underwater Acoustic Communication Channel*, Massachusetts Institute of Technology, Sep. 2006.

[10] E. A. P. Habets, S. Gannot, *Generating sensor signals in isotropic noise fields*, School of Engineering, Bar-Ilan University, Ramat-Gan, Israel, 27 September 2007.

[11] E. A. P. Habets, I. Cohen, S. Gannot, *Generating nonstationary multisensor signals under a spatial coherence constraint*, School of Engineering, Bar-Ilan University, Ramat-Gan, Israel, 20 August 2008.

[12] H. Cox, *Spatial correlation in arbitrary noise fields with application to ambient sea noise*, University of California, San Diego, 30 April 1973.